

A&A manuscript no.  
(will be inserted by hand later)

Your thesaurus codes are:  
20(10.15.1; 10.15.2 NGC 6994; 03.20.1)

ASTRONOMY  
AND  
ASTROPHYSICS

# CCD photometry in the region of NGC 6994: the remains of an old open cluster \*

L. P. Bassino \*\*, S. Waldhausen \*\*\*, and R. E. Martínez \*\*\*

Facultad de Ciencias Astronómicas y Geofísicas de la Universidad Nacional de La Plata and CONICET, Argentina.  
Observatorio Astronómico de la UNLP, Paseo del Bosque s/n, 1900–La Plata, Argentina.  
email: lbassino@fcaglp.fcaglp.unlp.edu.ar

Received / Accepted

**Abstract.** We present the results of  $BV(RI)_{KC}$  CCD photometry down to  $V = 21$  mag in the region of NGC 6994. To our knowledge, no photometry has previously been reported for this object and we find evidences that it is a poor and sparse old open cluster, with a minimum angular diameter of 9 arcmin, i.e. larger than the 3 arcmin originally assigned to it.

We obtain a color excess  $E_{B-V} = 0.07 \pm 0.02$  mag by means of the  $BVI_C$  technique. Based on the theoretical isochrones from Vandenberg (1985) that are in better agreement with our data, we estimate for this cluster a distance from the Sun of 620 pc ( $V_0 - M_V = 9 \pm 0.25$  mag) and an age lying within the range of 2 – 3 Gyr, adopting solar metallicity. Thus, the corresponding cluster's Galactocentric distance is 8.1 kpc and is placed at about 350 pc below the Galactic plane. According to this results, NGC 6994 belongs to the old open cluster population located in the outer disk and at large distances from the Galactic plane, and must have suffered significant individual dynamical evolution, resulting in mass segregation and evaporation of low mass stars.

**Key words:** open clusters and associations: general – open clusters and associations: individual: NGC 6994 – Techniques: image processing

## 1. Introduction

Open clusters are very useful for many purposes concerning our galaxy's structure and evolution; the oldest ones (with ages of about 1 Gyr or greater) are particularly suitable for studying the Galactic disk. As pointed out by Janes & Phelps (1994), the spatial distributions of old and young open clusters are notably different: the old ones, projected onto the Galactic plane, are located in the outer disk, at distances greater than 7.5 kpc from the Galactic center, towards the Galactic anticenter, whereas the young open clusters are distributed symmetrically about the Sun. The scale-heights estimated by fitting exponential laws to their respective distributions perpendicular to the Galactic plane, indicate that the old open cluster population (scale-height of 375 pc) is considerably thicker than the young one (scale-height of 55 pc). This distribution of old open clusters can be understood in terms of their dynamical evolution, as the fact of remaining in the outer disk and far from the Galactic plane, helps them to avoid tidal encounters with giant molecular clouds, mostly present in the inner disk, as well as the effect of other disruptive forces (Friel 1995 and references therein).

NGC 6994 (C2056–128) is an object located at low galactic latitude ( $\alpha = 20^h58^m9$ ,  $\delta = -12^\circ38'$  (J2000.0);  $l = 35^\circ7$ ,  $b = -34^\circ$ ), in Aquarius, and it has been very little studied. Collinder (1931) estimated for it a distance of 3.8 kpc, an angular diameter of 2.8 arcmin and wondered whether it was an open or globular cluster. Ruprecht (1966) classified NGC 6994 as a Trumpler (1930) class IV 1 p, a very sparse and poor open cluster. In a statistical analysis of Galactic clusters' ages, Wielen (1971) included it in the group of old and nearby ones, with high values of galactic latitude, but again considering it as a doubtful open cluster.

As far as we know, there have been no previous photometric studies of NGC 6994. Our investigation attempts to shed light on the nature of this object by means of CCD photometry, determining its probable members and true extension, and estimating its reddening, distance, age and metallicity. We also include a comparison with a model of

Send offprint requests to: L. P. Bassino

\* Table 1 is only available in electronic form at the CDS via anonymous ftp to cdsarc.u-strasbg.fr (130.79.128.5) or via <http://cdsweb.u-strasbg.fr/Abstract.html>

\*\* Member of the Carrera del Investigador Científico del Consejo Nacional de Investigaciones Científicas y Técnicas (CONICET), Argentina.

\*\*\* Visiting Astronomer, Complejo Astronómico El Leoncito operated under agreement between the CONICET (Argentina) and the National Universities of La Plata, Córdoba and San Juan

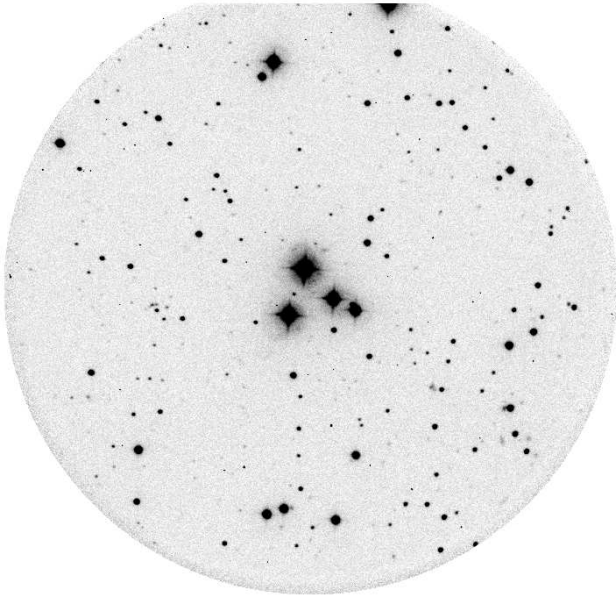


**Fig. 1.** CCD B image of the total area observed for NGC 6994. North is up and east is to the left. The diameter of the field is 9.6 arcmin and the exposure time is 6 min.

the Galactic stellar distribution that lends support to our observational results.

Sect. 2 describes observations and data reduction. Membership and the fundamental parameters of the cluster are discussed in Sect. 3. In Sect. 4 we present a comparison with a model of the Galaxy, and in Sect. 5 an analysis of the radial distribution. Our conclusions and a summary of the results are provided in the final Sect.

## 2. Observations and reductions

Observations for this project were carried out on the nights 12/13 and 13/14 October 1996, using the 2.15 m telescope at the Complejo Astronómico El Leoncito (CASLEO) in San Juan, Argentina. Direct CCD images were collected with a TEK 1024 chip and  $BV(RI)_{KC}$  filters; a focal reducer was attached to the telescope so that the scale was 0.8 arcsec/pixel, providing a circular usable field with a diameter of 9.6 arcmin. In each filter, a set of two frames in at least three different exposures were obtained for NGC 6994, as well as 40 frames of three Landolt (1992) fields containing 12 standard stars, which cover a range in color from  $(B-V) = -0.339$  to 1.551. The seeing ranged from 1.8 to 2.4 arcsec during both nights.

A blue CCD image is shown in Fig. 1 and it is evident from it that, formerly, the cluster was supposed to consist of just the four central brightest stars. The stellar distribution on the frame is presented in Fig. 2, which can be used as a finding chart and where we have included a 3 arcmin circle about the aforementioned brightest stars.

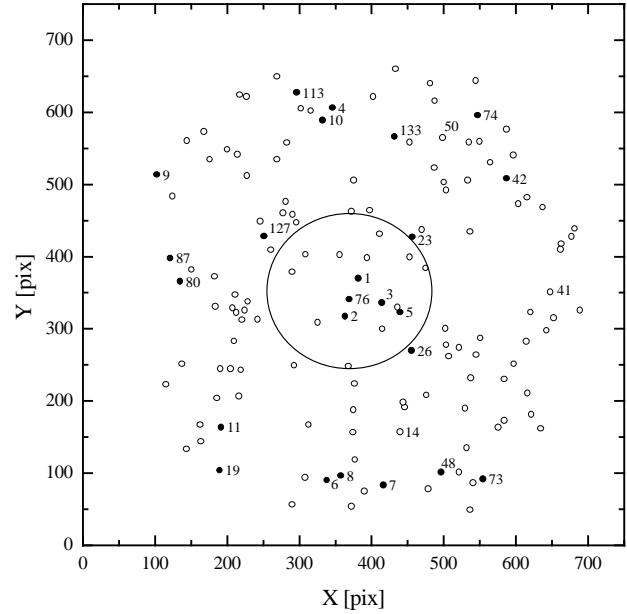


**Fig. 2.** Identification of the stars included in this study. The coordinates are in pixel units (0.8 arcsec/pixel). Member candidates are indicated by filled circles and their corresponding numbers. The central circle has a diameter of 3 arcmin.

All reductions were performed using IRAF<sup>1</sup>. Preliminary processing was done in the standard way; frames were trimmed, bias subtracted and flat-fielded using dome flats. Instrumental magnitudes of stars in the region of NGC 6994 were derived with the DAOPHOT package (Stetson 1987), a position dependent point spread function (PSF) and the corresponding aperture corrections were calculated for each frame, which were reduced separately. Standard stars were measured using aperture photometry and the following transformation equations were applied to transform our instrumental magnitudes

$$b = V + (B - V) + 3.180 + 0.275X - 0.129(B - V)$$

$$v = V + 1.911 + 0.165X + 0.067(B - V)$$

$$r = V - (V - R) + 1.796 + 0.115X - 0.033(V - R)$$

$$i = V - (V - I) + 2.775 + 0.075X - 0.101(V - R)$$

where lower case letters refer to instrumental magnitudes and upper case ones represent standard system values,  $X$  is the airmass, and the extinction coefficients were taken from Minniti et al. (1989). The rms error in the fits of all the transformation equations was of the order of 0.01 mag.

<sup>1</sup> IRAF is distributed by the National Optical Astronomy Observatories, which is operated by the Association of Universities for Research in Astronomy, Inc., under contract to the National Science Foundation.

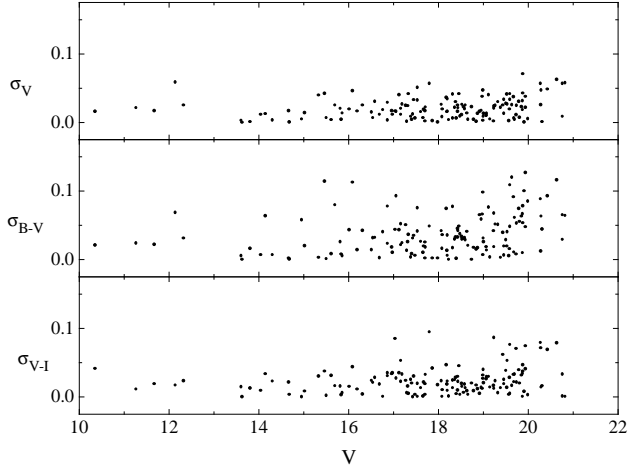


**Fig. 3.** Colors and  $V$  magnitude photometric errors as a function of  $V$  magnitude.

We finally calculated, for the 144 stars measured in this field, mean values for their colors and magnitudes weighted according to the photometric errors given by DAOPHOT, and the corresponding errors of the means which are shown in Fig. 3 as a function of  $V$  magnitude. The full photometric data set is listed in Table 1, where the  $X$  and  $Y$  coordinates are given in units of CCD pixels.

### 3. Results

Figs. 4, 5, and 6 show the color-magnitude diagrams (CMDs) for all the stars studied in the region of NGC 6994. We have made no attempt to eliminate the field stars because we lack a comparison field and we had no conclusive proof that the probable cluster did not extend out of the limits of the frame. A comparison with a model of our Galaxy for this field, which is discussed in the next Sect., will help to settle the question.

Membership, reddening and distance were determined together, following a kind of iterative process. Even though without radial velocities or metallicities we cannot confirm membership, we attempted to identify likely cluster members based on the locus of the stars in the  $(B - V)$  vs  $V$  diagram. We started by assuming that only stars in the central group, that is within the 3 arcmin circle (see Fig. 2), were members of the cluster. In the following steps, once we had estimations of color excess and distance modulus, we selected and added as member candidates those stars lying within  $\pm 2\epsilon$  of the Zero Age Mean Sequence (ZAMS) from Schmidt-Kaler (1982), shifted according to these chosen reddening and distance modulus ( $\epsilon$  being the internal error of the photometry), and we also included those lying within 0.75 mag of the upper envelope in case any of the member candidates were binaries (see Fig. 4). The reddening was estimated by means

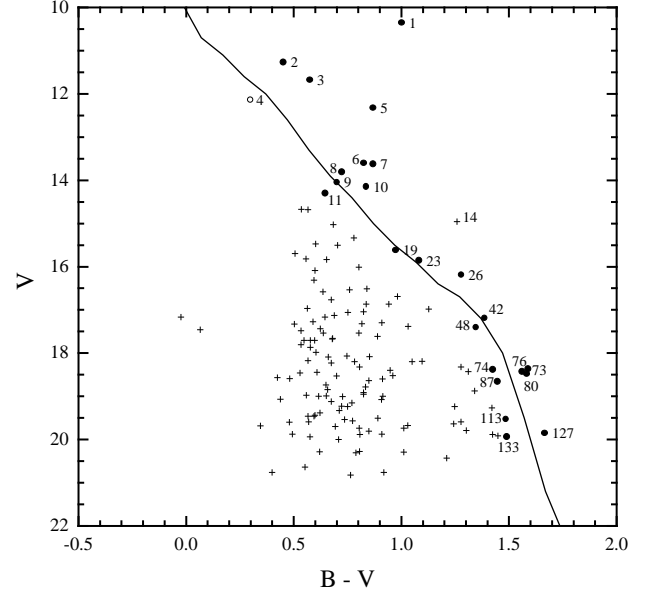


**Fig. 4.**  $V$  vs  $(B - V)$  color-magnitude diagram for all the stars studied in the region of NGC 6994. Member candidates are indicated by filled circles, a probable member by an open circle and nonmembers by crosses. The solid line is the Zero Age Mean Sequence (ZAMS) from Schmidt-Kaler (1982) shifted according to  $E(B - V) = 0.07$  mag and  $V - M_V = 9.2$  mag.

of the  $BVI_C$  technique, discussed by Cousins (1978), using the  $[(B - V) - (V - I)]$  vs  $(V - I)$  diagram (Fig. 7); member candidates with  $(V - I)$  colors between 0.5 and 1 mag were preferred for this determination because this color range is the most sensitive to the reddening in this diagram, as pointed out by Barrado & Byrne (1995). Finally, the distance modulus was chosen so as to obtain the best possible fit of the isochrones from the work of Vandenberg (1985) to our data, taking into account the already estimated color excess; the isochrones fitting also gave us information on the probable metallicity and age of the cluster. The whole procedure was repeated until no new member candidates were added to the group.

The final selection of member candidates was performed checking also their positions in the other CMDs. Star #4, though located slightly to the left of the sequences in the CMDs, was considered as a probable member because the errors in its mean  $\langle V \rangle$  and  $\langle B - V \rangle$  values (0.06 and 0.07 mag, respectively), were higher than for other stars of similar magnitude. Star #14 was considered as a field star. Stars #6 and #7 lie in the binary sequence, about 0.7 mag above the main sequence. In this way, a total of 24 members, including star #4, are proposed as belonging to this cluster: 7 of them are located within the central 3 arcmin circle, and another 17 stars are distributed out to the limits of our frames so that the true angular size of NGC 6994 might be even larger than 9 ar-

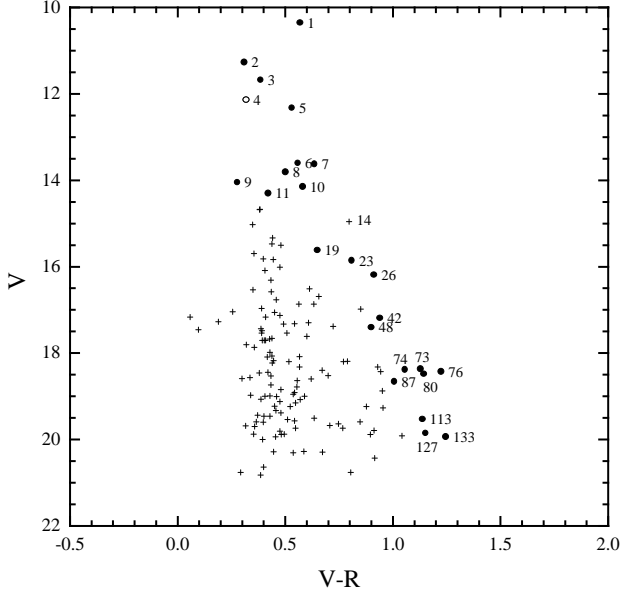


**Fig. 5.**  $V$  vs  $(V - R)$  color-magnitude diagram. Symbols as in Fig. 4.

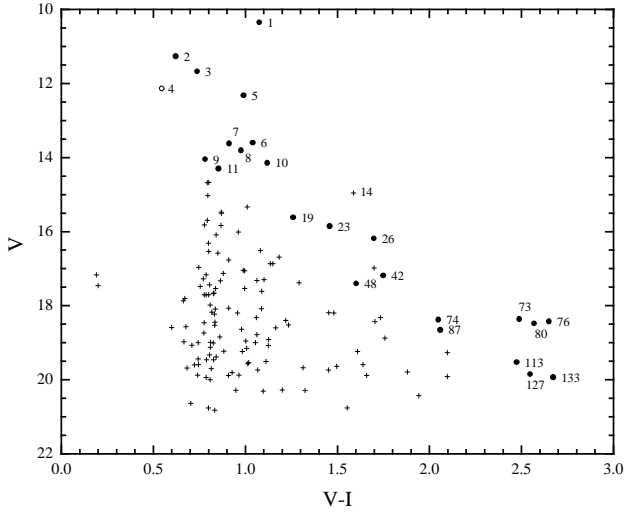


**Fig. 6.**  $V$  vs  $(V - I)$  color-magnitude diagram. Symbols as in Fig. 4.

cmin. Member star candidates are shown as filled circles in all the CMDs, the probable member #4 as an open circle and field stars as crosses. It is interesting to note that all stars in the CCD frames brighter than  $V = 14.5$  mag, i.e. the 11 brightest stars, seem to be members of NGC 6994.

The adopted reddening is  $E(V - I) = 0.09 \pm 0.03$  mag, and by means of the relation of Dean et al. (1978) we get  $E(B - V) = 0.07 \pm 0.02$  mag. The shift of the Cousins' sequence to the position shown in Fig. 7 proved to be relatively uncertain although, according to the direction of the reddening line, it was the best fitting that could be

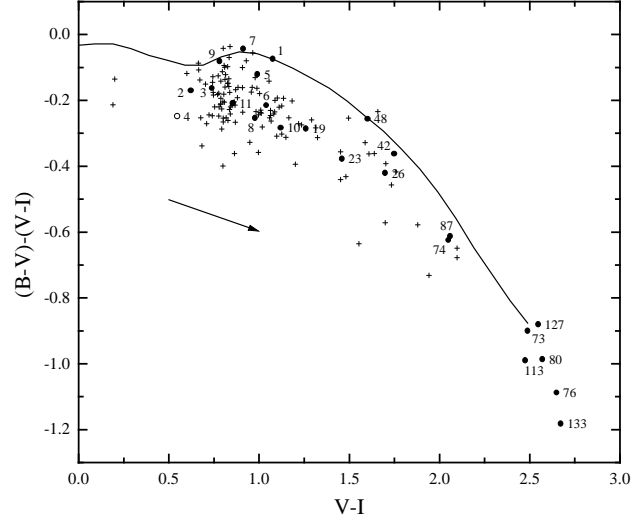


**Fig. 7.**  $[(B - V) - (V - I)]$  vs  $(V - I)$  color-color diagram. Symbols as in Fig. 4. The solid line is the intrinsic sequence for dwarfs (Cousins 1978) shifted according to the adopted color excess  $E(V - I) = 0.09$  mag. The arrow is the reddening line.

accomplished including member candidates with  $(V - I)$  colors between 0.5 and 1 mag, as explained above. Consequently, we decided to check the color excess and to obtain other estimates of the reddening from the maps of Burstein & Heiles (1982) and the recently published ones of Schlegel et al. (1998). In the former maps, the position corresponding to the galactic coordinates of the cluster is very close to the contour of  $E(B - V) = 0.06$  mag, and we obtained values ranging between 0.05 and 0.06 mag within the boundaries of our frames. The more reliable maps from Schlegel et al. gave  $E(B - V)$  between 0.04 and 0.06 mag for the same region. Thus, the estimates of reddening from both maps are in agreement, within the errors, with our previous determination so we decided to keep that color excess as the most accurate value and use it as a constraint in the isochrone fitting process.

In order to estimate the distance modulus we considered theoretical Vandenberg isochrones of different metallicities and ages, shifted according to the  $E(B - V)$  color excess. Isochrones of metallicity  $[\text{Fe}/\text{H}] = -0.45$  and more metal poor were inconsistent with our data for all ages. The  $-0.23$  dex ones at ages 2 – 3 Gyr provided a proper fit for a distance modulus  $(V - M_V) \approx 9.3$  mag, and the best global fit was obtained with the isochrones of solar metallicity corresponding to the same ages, at a  $(V - M_V) = 9.2 \pm 0.25$  mag. Due to the small number of stars involved in the fit we cannot discard the metallicity  $[\text{Fe}/\text{H}] = -0.23$ , but both distance moduli are in agreement within the errors, so we finally assumed that the distance derived with the solar metallicity isochrones was the most accurate one (Fig. 8).

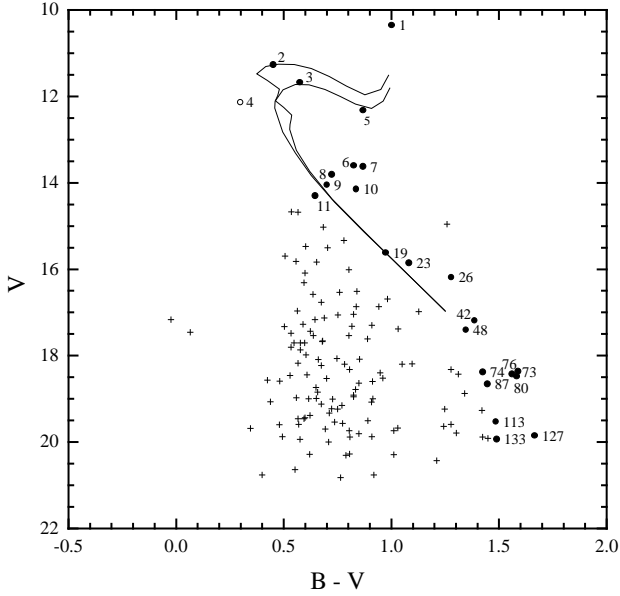


**Fig. 8.** Superposition of the CMD of Fig. 4 with the isochrones for solar metallicity and ages of (left to right): 2 and 3 Gyr (VandenBerg 1985). The isochrones are shifted according to  $E(B-V) = 0.07$  mag and  $V - M_V = 9.2$  mag.

If we adopt a value of  $R = A_V/E(B-V) = 3.2$ , we obtain an unreddened distance modulus of  $(V_0 - M_V) \approx 9 \pm 0.25$  mag, corresponding to a distance from the Sun of approximately  $d = 620$  pc. Taking into account its galactic latitude and assuming a solar Galactocentric distance of 8.5 kpc, we determine that NGC 6994 is located at about 350 pc below the Galactic plane and has a Galactocentric distance of about  $R_{gc} = 8.1$  kpc.

The two stars on the left side of the CMDs, which are identified as #41 and #50 in Fig. 2 and Table 1, deserve further discussion. According to their  $(B-V)$  colors they might be white dwarfs; it is thus worth to find out, by means of models, whether they are cluster white dwarfs candidates or not. We used the photometric calibration from Bergeron et al. (1995). The first step was to estimate the visual absolute magnitude for these stars assuming that they were located at the same distance as the cluster ( $M_V = 7.7-8.5$  mag, taking into account the error of the distance modulus); then, we obtained all the corresponding  $(B-V)$  colors and ages from the calibrations, including the models for the pure hydrogen and pure helium compositions as well as the ones for different values of the surface gravity. The model  $(B-V)$  colors range from  $-0.17$  to  $-0.33$  mag, that is, quite different from the observed ones (see Table 1); and if we look at the corresponding ages, they would be younger than  $10^7$  yr, which seems unlikely for the sparse cluster that we are dealing with. On the other side, the absolute magnitudes from the models that correspond to the observed  $(B-V)$  are

$M_V \leq 9.5$  mag, which differ in at least 1 mag from the ones obtained from the observations. We are then lead to conclude that stars #41 and #50 are not cluster white dwarfs. They may be either field white dwarfs or another type of blue object.

#### 4. Comparison with a Galactic model

In order to confirm the identification of the member star candidates as an old cluster, we attempted a comparison of our observational results with Galaxy model predictions. If we obtain, for the particular field we are studying, a theoretical distribution of field stars that matches the observed one, we will be quite confident on the nature of the sequence drawn by the member candidates as a cluster.

We obtained the star distribution predicted by the Galactic model from Reid & Majewski (1993), corresponding to a field of the same size, located at the same position as NGC 6994, and including stars up to the same  $V$  limiting magnitude. Due to the low value of the galactic latitude, we expected to find, as field star contamination, several stars from the thick disk and from the halo added to the ones belonging to the Galactic disk. Figs. 9 and 10 show the theoretical  $V$  vs  $(B-V)$ , and  $V$  vs  $(V-I)$  CMDs, reddened according to the values obtained in the previous Sect., and where we have included the sequence of member stars to perform a better comparison with Figs. 4 and 6, respectively. We can see that the model and the observed CMDs appear very similar, with a high proportion of stars from the thick disk and the halo; and that the candidate cluster members are located on an separate sequence, away from the field stars. The same effect is present in the  $V$  vs  $(V-R)$  CMD, which is not shown. We believe that this comparison is giving strong support to the identification of the cluster star candidates as members of a genuine open cluster.

By means of this comparison of the observations with the model predictions, we can see that, up to the limiting  $V$  magnitude of the stars involved in this paper ( $V = 21$  mag), all the stars redder than  $(V-I) = 1.5$  mag belong to the disk population without any contribution from the halo (see Fig. 10). This fact has already been pointed out by Reid et al. (1996), in their analysis of two deep and relatively high galactic latitude fields.

#### 5. Stellar radial distribution

Given the small number of member candidates of NGC 6994, it is worth computing the surface density of stars in the region studied. Taking as a rough center the position of the four brightest stars, that is, the center of the 1.5 arcmin radius circle in Fig. 2, we calculated the cumulative projected number density within a series of concentric annular rings about such point. It is displayed in Fig. 11 which shows that NGC 6994 presents an increase of the density towards the center. Anyway, as this distribution

represents an important proof of the existence of the cluster, it should be analyzed in a statistical way. By means of a random number generator we made a set of 10 uniform distributions of the same number of stars, scattered across the same area, and then applied a Kolmogorov-Smirnov test (Press et al. 1992) to prove if they were statistically different from the observed stellar radial distribution. The statistic in this analysis is the maximum vertical separation between the observed and each random cumulative distributions, and  $P$  is the corresponding significance level for the hypothesis that the two samples are drawn from the same parent distribution. The probabilities  $P$  obtained, in sorted order, were of 0.151, 0.141, and the rest ranged from 0.045 to 0.003; these results show that the observed distribution is significantly different from the uniform distributions and that it has not occurred just by chance. In this way, the existence of the cluster as a true identity is enhanced, and it should also be noticed that it is highly likely that the outer members of the cluster are located out of the bounds of our CCD frames.

## 6. Conclusions

The results of our photometry and the comparison with a Galactic model suggest that NGC 6994 is an old and sparse open cluster. We identify only 24 member candidates within the limits of our CCD frames, including the four brightest members that are located close to the center. The best isochrone fits give an age that lies within

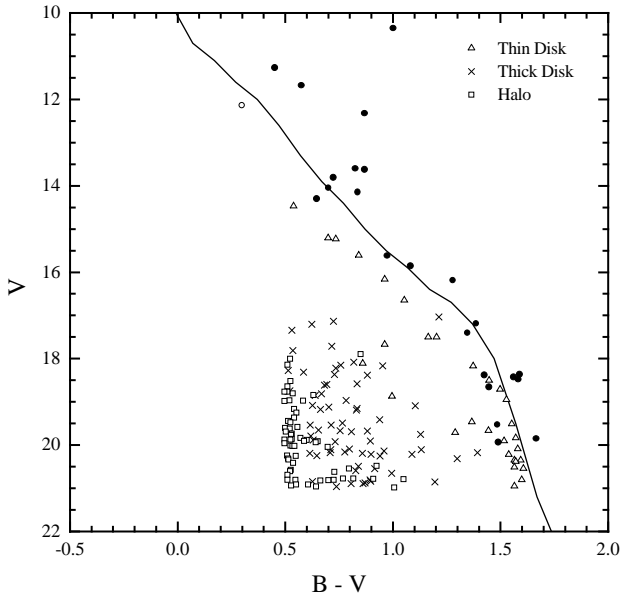


**Fig. 9.**  $V$  vs  $(B - V)$  color-magnitude diagram from the Reid & Majewski (1993) Galactic model corresponding to the region under study, plotted together with the NGC 6994 member candidates and the ZAMS (indicated as in Fig. 4).

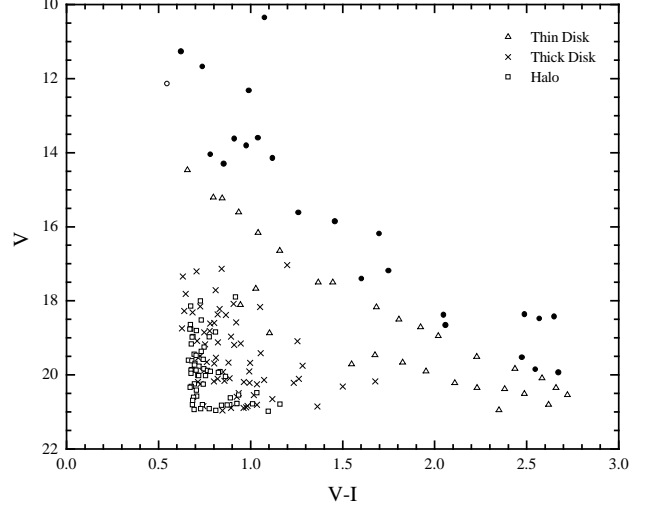


**Fig. 10.**  $V$  vs  $(V - I)$  color-magnitude diagram from the Reid & Majewski (1993) Galactic model corresponding to the region under study, plotted together with the NGC 6994 member candidates. Symbols as in Fig. 9.

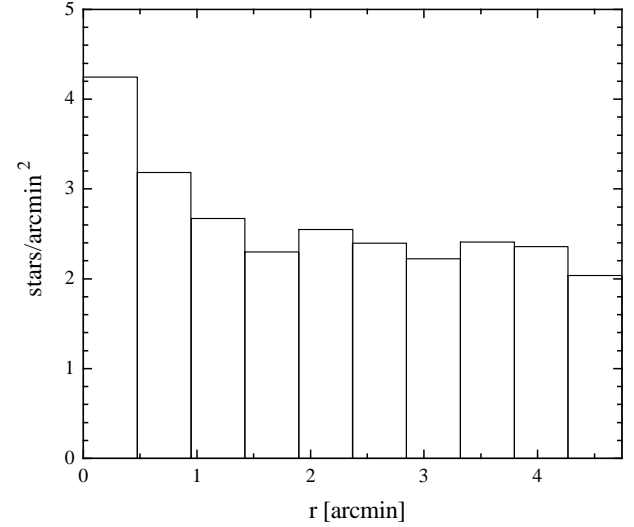


**Fig. 11.** Stellar surface density in the region of NGC 6994 as a function of distance to the center.

the range of 2 to 3 Gyr, assuming solar metallicity. The distance of the cluster from the Sun is estimated as 620 pc and the Galactocentric distance as 8.1 kpc; it is situated about 350 pc below the Galactic plane.

Our interpretation of the above results is based on the dynamical evolution of the cluster. Friel (1995) discussed the distribution of old open clusters projected on the Galactic plane and perpendicular to it. All the old open clusters present Galactocentric distances larger than 7.5 kpc and their distribution with height from the plane

is much broader than for the young ones, that is, the old cluster population can be fitted by a 375 pc scale-height exponential compared to the 55 pc scale-height of clusters with ages less than the Hyades (Janes & Phelps 1994). Both facts are in favour of the cluster longevity: the giant molecular clouds, whose encounters with open clusters can be devastating (Terlevich 1987), are mainly located in the inner disk.

On the other side, clusters older than 1 Gyr are expected to present considerable mass segregation. They have had enough time to relax dynamically so that more massive stars end up centrally concentrated, and low mass stars have moved to the outer regions and may have escaped from the cluster. This process of evaporation is experienced by isolated clusters but is more efficient in the presence of an external field due to the host galaxy; this seems to have happened to a high proportion of NGC 6994 low mass members.

Finally, it is interesting to note the N-body simulations from Terlevich (1987) showed that, after 300–400 Myr of evolution, some of the stars remained around each open cluster, forming an extended corona outside King’s tidal radius, but being still linked to the cluster. We find a similar kind of corona in the outskirts of NGC 6994, formed by stars that are likely to escape in the near future.

*Acknowledgements.* The authors acknowledge use of the CCD and data acquisition system supported under U. S. National Science Foundation grant AST-90-15827 to R. M. Rich. We are greatly indebted to T. von Hippel for making many useful suggestions which improved this paper, and for providing the code for the Galactic model calculations. We are also grateful to H. G. Marraco for his discussions and advice and for reading the manuscript, and to A. Feinstein and D. D. Carpintero for their comments. Thanks are due to S. D. Abal de Rocha, M. C. Fanjul de Correbo and E. Suárez for their technical assistance. This work was supported by grants from La Plata University and from the CONICET.

## References

- Barrado, D. and Byrne, P. B., 1995, A&AS 111, 275  
 Bergeron, P., Wesemael, F. and Beauchamp, A., 1995, PASP 107, 1047  
 Burstein, D. and Heiles, C., 1982, AJ 87, 1165  
 Collinder, P., 1931, Ann. Obs. Lund 2  
 Cousins, A. W. J., 1978, MNASSA 37,62.  
 Dean, J. F. , Warren, P. R., and Cousins, A. W. J., 1978, MNRAS 183, 569  
 Friel, E. D., 1995, ARA&A, 33,381  
 Janes, K. A. and Phelps, R. L., 1994, AJ 108, 1773  
 Landolt, A. U., 1992, AJ 104, 340  
 Minniti, D. , Clariá, J. J. and Gómez, M. N., 1989, Ap&SS 158, 9  
 Press, W. H., Teukolsky, S. A., Vetterling, W. T. and Flannery, B. P. 1992, Numerical Recipes-2nd ed., Cambridge University Press, Cambridge  
 Reid, I. N. and Majewski, S. R., 1993, ApJ 409, 635  
 Reid, I. N., Yan, L., Majewski, S., Thompson, I. and Smail, I. 1996, AJ 112, 1472  
 Ruprecht, J., 1966, Bull. Astr. Inst. Csl. 17, 33  
 Schmidt-Kaler, Th. 1982, in Astrophysical Data I: Planets and Stars, K. R. Lang (ed.), Springer-Verlag, New York  
 Schlegel, D. J. , Finkbeiner, D. P. and Davis, M., 1998, ApJ 500, 525  
 Stetson, P. B., 1987, PASP 99, 191  
 Terlevich, E., 1987, MNRAS 224, 193  
 Trumpler, R. J., 1930, Lick Obs. Bull. 14, 154  
 VandenBerg, D. A., 1985, ApJS 58, 711  
 Wielen, R., 1971, A&A 13, 309

**Table 1.** BVRI photometry for 144 stars in the region of NGC 6994

Star	X	Y	RA(J2000.0)	Dec(J2000.0)	V	B-V	V-R	V-I
1	381.72	369.95	20 58 56.8	-12 38 29	10.355	1.002	0.570	1.076
2	363.57	317.24	20 58 57.8	-12 37 45	11.269	0.452	0.309	0.622
3	414.42	335.88	20 58 54.8	-12 38 04	11.675	0.575	0.386	0.738
4	346.23	606.07	20 58 59.8	-12 41 43	12.142	0.298	0.319	0.547
5	439.63	322.71	20 58 53.5	-12 37 54	12.322	0.870	0.531	0.991
6	338.02	89.84	20 58 58.3	-12 34 35	13.605	0.825	0.559	1.040
7	416.68	83.22	20 58 53.8	-12 34 35	13.626	0.869	0.635	0.913
8	357.53	96.16	20 58 57.2	-12 34 42	13.809	0.724	0.502	0.978
9	102.48	513.39	20 59 13.3	-12 40 12	14.047	0.701	0.277	0.782
10	332.59	588.62	20 59 00.5	-12 41 28	14.150	0.837	0.581	1.120
11	191.47	163.21	20 59 06.8	-12 35 28	14.303	0.647	0.421	0.855
12	614.67	282.16	20 58 43.4	-12 37 31	14.670	0.536	0.382	0.801
13	439.62	157.07	20 58 52.8	-12 35 38	14.679	0.567	0.381	0.793
14	637.50	468.42	20 58 42.7	-12 40 05	14.959	1.258	0.796	1.587
15	615.91	482.14	20 58 44.0	-12 40 16	15.026	0.684	0.349	0.796
16	487.60	615.60	20 58 51.8	-12 42 00	15.336	0.780	0.441	1.010
17	616.05	210.81	20 58 43.0	-12 36 31	15.470	0.602	0.439	0.868
18	452.69	399.34	20 58 53.0	-12 38 58	15.502	0.703	0.479	0.871
19	189.43	104.01	20 59 06.7	-12 34 39	15.616	0.974	0.649	1.260
20	642.57	297.65	20 58 41.8	-12 37 44	15.698	0.506	0.354	0.793
21	260.59	409.18	20 59 03.9	-12 38 55	15.818	0.557	0.397	0.778
22	368.31	248.08	20 58 57.2	-12 36 47	15.834	0.652	0.443	0.867
23	456.52	427.18	20 58 52.9	-12 39 22	15.856	1.082	0.809	1.459
24	214.24	541.21	20 59 07.0	-12 40 42	16.011	0.802	0.475	0.962
25	137.50	251.30	20 59 10.2	-12 36 38	16.092	0.599	0.406	0.840
26	455.32	269.74	20 58 52.4	-12 37 11	16.191	1.278	0.913	1.699
27	452.85	558.41	20 58 53.5	-12 41 09	16.314	0.594	0.432	0.799
28	414.90	299.83	20 58 54.7	-12 37 33	16.509	0.839	0.613	1.081
29	621.61	181.32	20 58 42.6	-12 36 08	16.538	0.759	0.350	0.801
30	534.91	558.18	20 58 48.9	-12 41 14	16.585	0.636	0.435	0.851
31	530.10	189.63	20 58 47.8	-12 36 10	16.688	0.982	0.656	1.183
32	182.66	372.40	20 59 08.2	-12 38 21	16.766	0.674	0.458	0.910
33	564.68	530.49	20 58 47.1	-12 40 53	16.865	0.942	0.633	1.135
34	540.77	86.31	20 58 46.8	-12 34 45	16.869	0.836	0.562	1.149
35	603.49	473.07	20 58 44.7	-12 40 07	16.963	0.563	0.389	0.747
36	290.05	56.45	20 59 00.8	-12 34 05	16.981	1.127	0.850	1.699
37	634.78	161.44	20 58 41.8	-12 35 51	17.040	0.824	0.256	0.988
38	689.12	325.61	20 58 39.3	-12 38 10	17.060	0.752	0.450	0.996
39	549.76	559.27	20 58 48.1	-12 41 15	17.125	0.688	0.475	0.880
40	281.08	476.07	20 59 02.9	-12 39 51	17.163	0.646	0.409	0.788
41	647.72	350.78	20 58 41.7	-12 38 29	17.163	-0.023	0.058	0.190
42	587.40	508.21	20 58 45.8	-12 40 36	17.190	1.387	0.940	1.750
43	536.56	49.08	20 58 46.1	-12 34 12	17.274	0.589	0.190	0.771
44	216.58	206.71	20 59 05.7	-12 36 05	17.294	0.908	0.608	1.101
45	296.23	446.98	20 59 02.2	-12 39 27	17.319	0.817	0.543	1.063
46	544.57	643.63	20 58 48.6	-12 42 25	17.331	0.503	0.492	0.864
47	551.05	286.92	20 58 47.0	-12 37 31	17.383	1.032	0.723	1.291
48	496.72	101.38	20 58 49.3	-12 34 53	17.407	1.346	0.900	1.603
49	150.47	381.65	20 59 10.0	-12 38 27	17.433	0.624	0.387	0.805
50	498.57	564.61	20 58 51.0	-12 41 17	17.456	0.065	0.096	0.200
51	242.05	312.93	20 59 04.6	-12 37 35	17.485	0.534	0.391	0.754
52	436.11	329.65	20 58 53.7	-12 38 00	17.533	0.638	0.508	0.995
53	144.47	560.32	20 59 11.1	-12 40 53	17.534	0.802	0.390	0.838
54	227.62	512.14	20 59 06.1	-12 40 19	17.609	0.889	0.600	1.088
55	376.95	118.76	20 58 56.2	-12 35 02	17.662	0.680	0.438	0.828
56	475.29	384.11	20 58 51.7	-12 38 46	17.676	0.678	0.426	0.827



**Table 1.** continued

Star	X	Y	RA(J2000.0)	Dec(J2000.0)	V	B-V	V-R	V-I
57	521.22	101.06	20 58 47.9	-12 34 55	17.705	0.576	0.392	0.787
58	290.20	378.61	20 59 02.0	-12 38 31	17.707	0.547	0.409	0.801
59	537.86	231.95	20 58 47.6	-12 36 45	17.708	0.597	0.403	0.776
60	620.35	322.74	20 58 43.2	-12 38 03	17.802	0.533	0.320	0.671
61	575.68	163.49	20 58 45.1	-12 35 49	17.864	0.577	0.356	0.663
62	374.85	187.40	20 58 56.5	-12 35 58	17.985	0.603	0.429	0.808
63	176.11	534.48	20 59 09.1	-12 40 34	18.067	0.747	0.437	0.908
64	325.59	308.61	20 58 59.8	-12 37 35	18.081	0.852	0.566	1.087
65	124.47	483.47	20 59 11.9	-12 39 50	18.088	0.661	0.417	0.837
66	662.24	409.77	20 58 41.1	-12 39 18	18.177	0.566	0.446	0.818
67	470.04	436.94	20 58 52.2	-12 39 30	18.192	1.096	0.788	1.452
68	681.49	438.47	20 58 40.2	-12 39 43	18.199	1.050	0.770	1.481
69	282.83	557.82	20 59 02.6	-12 41 13	18.200	0.782	0.516	0.957
70	531.81	135.01	20 58 47.5	-12 35 24	18.226	0.674	0.439	0.832
71	186.10	203.63	20 59 07.3	-12 36 00	18.318	0.806	0.566	1.059
72	375.42	505.67	20 58 57.7	-12 40 22	18.320	1.277	0.929	1.734
73	554.82	91.59	20 58 46.0	-12 34 48	18.365	1.589	1.128	2.489
74	546.98	595.44	20 58 48.3	-12 41 46	18.385	1.425	1.056	2.049
75	376.59	223.98	20 58 56.6	-12 36 29	18.399	0.948	0.671	1.219
76	369.43	340.64	20 58 57.4	-12 38 04	18.428	1.561	1.224	2.650
77	268.94	649.45	20 59 04.3	-12 42 16	18.431	1.311	0.943	1.703
78	246.08	448.60	20 59 04.8	-12 39 28	18.440	0.607	0.419	0.836
79	481.13	640.13	20 58 52.2	-12 42 19	18.459	0.528	0.379	0.776
80	135.02	365.55	20 59 10.9	-12 38 13	18.482	1.584	1.143	2.570
81	290.85	458.19	20 59 02.4	-12 39 38	18.518	0.960	0.699	1.235
82	476.11	207.78	20 58 50.9	-12 36 22	18.529	0.699	0.434	0.833
83	212.79	322.22	20 59 06.2	-12 37 41	18.566	0.424	0.336	0.676
84	545.33	264.11	20 58 47.2	-12 37 11	18.586	0.482	0.299	0.600
85	199.96	548.06	20 59 07.8	-12 40 48	18.598	0.912	0.620	1.165
86	583.93	230.34	20 58 44.9	-12 36 45	18.635	0.849	0.555	0.979
87	121.02	397.87	20 59 11.8	-12 38 39	18.660	1.446	1.006	2.059
88	652.39	314.71	20 58 41.4	-12 37 58	18.740	0.649	0.433	0.774
89	372.20	53.86	20 58 56.2	-12 34 08	18.786	0.833	0.554	1.063
90	502.50	300.28	20 58 49.7	-12 37 38	18.841	0.657	0.480	0.861
91	411.28	431.56	20 58 55.4	-12 39 22	18.875	1.340	0.951	1.758
92	308.80	402.93	20 59 01.1	-12 38 53	18.915	0.824	0.543	1.126
93	220.81	312.33	20 59 05.8	-12 37 34	18.955	0.824	0.537	1.002
94	217.26	624.21	20 59 07.2	-12 41 50	18.976	0.558	0.339	0.666
95	587.50	576.09	20 58 46.0	-12 41 33	18.991	0.651	0.428	0.810
96	521.39	273.69	20 58 48.6	-12 37 18	18.996	0.914	0.589	1.055
97	374.54	156.50	20 58 56.5	-12 35 33	19.002	0.615	0.406	0.743
98	597.04	251.26	20 58 44.2	-12 37 04	19.009	0.727	0.459	0.825
99	390.38	74.61	20 58 55.2	-12 34 26	19.066	0.438	0.387	0.709
100	162.94	167.20	20 58 08.5	-12 35 30	19.072	0.908	0.569	1.125
101	662.98	417.55	20 58 41.1	-12 39 25	19.119	0.674	0.475	0.810
102	478.88	77.89	20 58 50.3	-12 34 33	19.148	0.770	0.548	1.006
103	277.32	460.27	20 59 03.1	-12 39 38	19.230	0.722	0.450	0.882
104	209.87	282.57	20 59 06.2	-12 37 08	19.235	1.247	0.877	1.609
105	433.23	659.82	20 58 55.0	-12 42 32	19.240	0.750	0.523	0.984
106	393.81	398.20	20 58 56.2	-12 38 55	19.268	1.420	0.954	2.098
107	596.59	540.46	20 58 45.3	-12 41 03	19.328	0.711	0.456	0.806
108	446.29	191.16	20 58 52.6	-12 36 05	19.386	0.622	0.480	0.842
109	677.35	427.87	20 58 40.3	-12 39 35	19.437	0.598	0.371	0.743
110	533.56	505.53	20 58 48.8	-12 40 30	19.462	0.567	0.401	0.828
111	204.63	244.42	20 59 06.4	-12 36 36	19.462	0.594	0.428	0.788
112	507.09	261.73	20 58 49.4	-12 37 07	19.504	0.891	0.635	1.111
113	296.31	627.41	20 59 02.7	-12 41 59	19.528	1.486	1.138	2.476

**Table 1.** continued

Star	X	Y	RA(J2000.0)	Dec(J2000.0)	V	B-V	V-R	V-I
114	444.03	197.81	20 58 52.7	-12 36 12	19.535	0.736	0.510	1.017
115	292.71	249.25	20 59 01.5	-12 36 44	19.569	0.773	0.543	1.012
116	207.53	328.43	20 59 06.6	-12 37 46	19.588	0.570	0.365	0.745
117	168.18	572.81	20 59 09.7	-12 41 06	19.591	1.277	0.848	1.639
118	500.22	502.82	20 58 50.6	-12 40 26	19.595	0.479	0.397	0.723
119	227.20	621.36	20 59 06.6	-12 41 50	19.638	1.242	0.747	1.496
120	487.28	523.10	20 58 51.4	-12 40 42	19.676	1.030	0.707	1.314
121	372.16	462.46	20 58 57.7	-12 39 46	19.683	0.345	0.316	0.683
122	503.31	277.80	20 58 49.6	-12 37 21	19.698	0.693	0.357	0.815
123	143.63	133.00	20 59 09.5	-12 35 01	19.734	0.804	0.547	1.067
124	115.59	222.78	20 59 11.4	-12 36 12	19.740	1.011	0.766	1.452
125	356.25	402.28	20 58 58.4	-12 38 55	19.791	1.301	0.913	1.880
126	224.28	325.72	20 59 05.5	-12 37 44	19.807	0.849	0.475	0.928
127	251.14	428.03	20 59 04.5	-12 39 11	19.852	1.667	1.151	2.548
128	397.87	464.01	20 58 56.3	-12 39 48	19.873	0.910	0.496	0.966
129	269.03	534.80	20 59 03.9	-12 40 41	19.874	0.494	0.354	0.741
130	316.22	602.08	20 59 01.4	-12 41 38	19.883	0.807	0.481	0.907
131	302.11	604.99	20 59 02.2	-12 41 40	19.884	1.424	0.896	1.658
132	503.67	491.99	20 58 50.4	-12 40 18	19.915	1.449	1.042	2.098
133	432.04	566.13	20 58 54.7	-12 41 14	19.937	1.490	1.245	2.672
134	190.82	244.36	20 59 07.2	-12 36 34	19.939	0.576	0.454	0.787
135	536.49	434.43	20 58 48.3	-12 39 30	19.996	0.709	0.394	0.809
136	211.07	347.25	20 59 06.3	-12 37 59	20.273	0.806	0.586	1.200
137	219.03	242.57	20 59 05.5	-12 36 36	20.284	0.621	0.446	0.948
138	312.83	167.07	20 59 00.0	-12 35 38	20.289	1.011	0.672	1.325
139	163.80	143.92	20 59 08.3	-12 35 11	20.310	0.789	0.537	1.097
140	402.41	621.69	20 58 56.6	-12 42 00	20.428	1.211	0.915	1.942
141	307.91	93.99	20 59 00.0	-12 34 37	20.636	0.552	0.399	0.702
142	184.07	330.57	20 59 07.8	-12 37 47	20.761	0.400	0.292	0.799
143	228.77	337.79	20 59 05.3	-12 37 54	20.762	0.918	0.804	1.553
144	583.95	173.00	20 58 44.7	-12 35 58	20.819	0.763	0.386	0.834

In all cases the number of observations is equal to 2